Journal of Biomolecular NMR, **12:** 307–318, 1998.
KLUWER/ESCOM

Identification of slow motions in the reduced recombinant high-potential iron sulfur protein I (HiPIP I) from *Ectothiorhodospira halophila* via ^{15}N rotating-frame NMR relaxation measurements

Lucia Banci*, Isabella C. Felli & Dionysios Koulougliotis
Department of Chemistry, University of Florence, Via G. Capponi 7, 50121 Florence, Italy

Received 21 January 1998; Accepted 15 April 1998

Key words: protein dynamics, nitrogen-15 NMR, rotating-frame relaxation

Abstract

Rotating-frame ^{15}N relaxation rate ($R_{1\rho}$) NMR experiments have been performed in order to study the dynamic behavior of the reduced recombinant high-potential iron-sulfur protein iso I (HiPIP I) from *Ectothiorhodospira halophila*, in the μs to ms time range. Measurements of $R_{1\rho}$ were perfomed as a function of the effective spin-lock magnetic field amplitude by using both on and off-resonance radio frequency irradiation. The two data sets provided consistent results and were fit globally in order to identify possible exchange processes in an external loop of the reduced HiPIP I. The loop consists of residues 43–45 and the correlation time of the exchange process was determined to be 50 ± 8 μs for the backbone nitrogen of Gln 44.

Introduction

An important step towards understanding the functional mechanism of a protein is the determination of its structure. Multidimensional NMR spectroscopy provides the means to achieve this task in solution and therefore in conditions as close as possible to the physiological ones. The technique has recently been extended to paramagnetic molecules (Banci et al., 1994; Banci and Pierattelli, 1995; Bertini and Felli, 1995; Bertini et al., 1996c). Indeed, the first NMR solution structure of a paramagnetic metalloprotein has been solved on a high-poterntial iron-sulfur protein (HiPIP hereafter) (Banci et al., 1994).

This class of relatively small (less than 10 kDa) proteins contains a single cubane-like Fe_4S_4 cluster and such proteins are commonly found in purple photoheterotrophic bacteria (Bartsch, 1978). A series of studies on the characterization of the electronic properties of the cluster have been done by using different biophysical techniques: Mössbauer (Moss et al., 1968; Dickson et al., 1974; Dickson et al., 1976; Middleton et al., 1980; Bertini et al., 1993a), electron paramagnetic resonance (EPR) (Led and Nesgard, 1987; Dunham et al., 1991; Hagen, 1992), electron nuclear double resonance (ENDOR) (Rius and Lamotte, 1989; Mouesca et al., 1991; Mouesca et al., 1993) and nuclear magnetic resonance (NMR) (Bertini et al., 1992a,b, 1991; Banci et al., 1993a,b). Recently, direct experimental evidence has been provided to show that HiPIPs participate in photosynthetic electron transfer (Hochkoeppler et al., 1995). Two oxidation states are easily accessible for the Fe_4S_4 cluster: the reduced state which contains four $Fe^{2.5+}$ ions (Carter et al., 1972; Middleton et al., 1980) and the oxidized state containing two $Fe^{2.5+}$ and two Fe^{3+} ions (Middleton et al., 1980; Bertini et al., 1993a). The HiPIP I from *Ectothiorhodospira halophila*, has been the subject of intense NMR investigation in our lab, in both oxidation states. Its small size (73 amino acids) and efficient expression in *Escherichia coli* (Eltis et al., 1994) have allowed the determination of the three dimensional structure in solution of both the reduced and oxidized forms by means of ^{1}H, ^{15}N and ^{13}C two and three-dimensional NMR spectroscopy (Banci et al., 1994; Bertini et al., 1996a, 1995, 1997). Thus, by close comparison of the two solution structures, one can account

*To whom correspondence should be addressed.

for the subtle structural rearrangements occuring upon electron transfer via the Fe_4S_4 cube.

After the structure of the protein has been made available, the next step in the effort to link protein structure with function is the study of protein dynamics. Dynamic properties of proteins in solution are nowdays commonly analyzed by measuring heteronuclear relaxation rates. However, the HiPIP I from *E. halophila* in the reduced state, even if it has an electronic ground spin state $S = 0$ (Middleton et al., 1980), is paramagnetic due to population of low-lying excited spin states that are accessible at room temperature. The paramagnetism severely enhances the nuclear relaxation rates causing the longitudinal relaxation rates (R_1) for protons close to the metal cluster to become as large as 300 Hz (Bertini et al., 1996a). These effects have already been examined in detail first by including the paramagnetic contribution in a relaxation matrix analysis of NOEs (Bertini et al., 1996b) and subsequently by measuring directly proton longitudinal relaxation rates (Bertini et al., 1996a). By using this knowledge it is possible to evaluate the distance from the paramagnetic center up to which the relaxation enhancement is significant and, in part, to account for this effect. In this work we are interested in probing protein motions that occur in a μs to ms timescale. This was achieved by measuring the amide backbone ^{15}N rotating-frame relaxation rate, $R_{1\rho}(= 1/T_{1\rho})$, by using off- and on-resonance RF irradiation.

The theoretical formulation of $R_{1\rho}$ and its importance for investigating exchange processes has long been recognized (A**br**agam, 1961; Deverell et al., 1970; Wennerström, 1972). Recently, there have been an increasing number of researchers who have used heteronuclear, on-resonance, $R_{1\rho}$ measurements in order to probe protein dynamics (Peng & Wagner, 1995; Szyperski et al., 1993; Tjandra et al., 1995; Habazettl et al., 1996). This is mainly due to the fact that $R_{1\rho}$ offers potentially different information about the spectral densities than either longitudinal and transverse relaxation rates or steady state NOEs. More specifically the dynamics in the μs to ms time regime can be probed (Davis et al., 1994). An estimation of the correlation time of the exchange process τ_{ex} can (in favourable cases) be achieved by relaxation measurements of $R_{1\rho}$ as a function of the strength of the spin-lock effective RF field.

The measurement of $R_{1\rho}$ can also be performed in the presence of an off-resonance RF field along a tilted magnetic field axis ($R_{1\rho}^{\mathrm{OFF}}$) (Jones, 1966; Jacquinot and Goldman, 1973; James et al., 1977, 1978; James and Sawan, 1979; Peng et al., 1991). Recently, a detailed theoretical and experimental study appeared on the contribution of rapid chemical exchange processes in off-resonance rotating-frame relaxation rate measurements in ^{1}H (Desvaux et al., 1995) and ^{15}N (Zinn-Justin et al., 1997) studies. In addition, an alternative way to use off-resonance $R_{1\rho}$ measurements in order to monitor macromolecular motions in the μs to ms time scale has been presented (Akke and Palmer, III, 1996).

In this work, on- and off-resonance measurements of $R_{1\rho}$ have been combined in order to probe 'slow' (μs to ms) internal motions in a biological system containing a paramagnetic center (the reduced form of HiPIP I). A protein loop in which an exchange process is operative is successfully identified and the correlation time for the motion is determined by a global fit of both on- and off- resonance $R_{1\rho}$ experimental values.

Materials and Methods

Sample Preparation

^{15}N labeled HiPIP I was isolated and purified from *E. coli* cultures grown in minimal M9 medium enriched with $(^{15}NH_4)_2SO_4$ (0.3 g/l). Approximately 10 mg of the purified protein was exchanged through ultrafiltration (YM3 membranes, Amicon) with 50 mM potassium phospate buffer at pH 5.0. The sample volume was concentrated to ∼ 450 μl and then the protein was reduced by adding 20 μl of 0.15 M buffered solution of sodium isoascorbate under anaerobic conditions. This resulted in a more than 95% reduced protein at an approximate final concentration of 2 mM. The oxidation state of the sample was checked periodically (approximately every 12 h) during the course of the experiments by recording 1D ^{1}H NMR spectra. The paramagnetically shifted signals of the oxidized and reduced froms of the protein have quite different chemical shifts and are clearly indicative of its oxidation state. All these 'control' spectra turned out to be practically identical with each other and also with that already reported for the reduced form of the protein (Bertini et al., 1994).

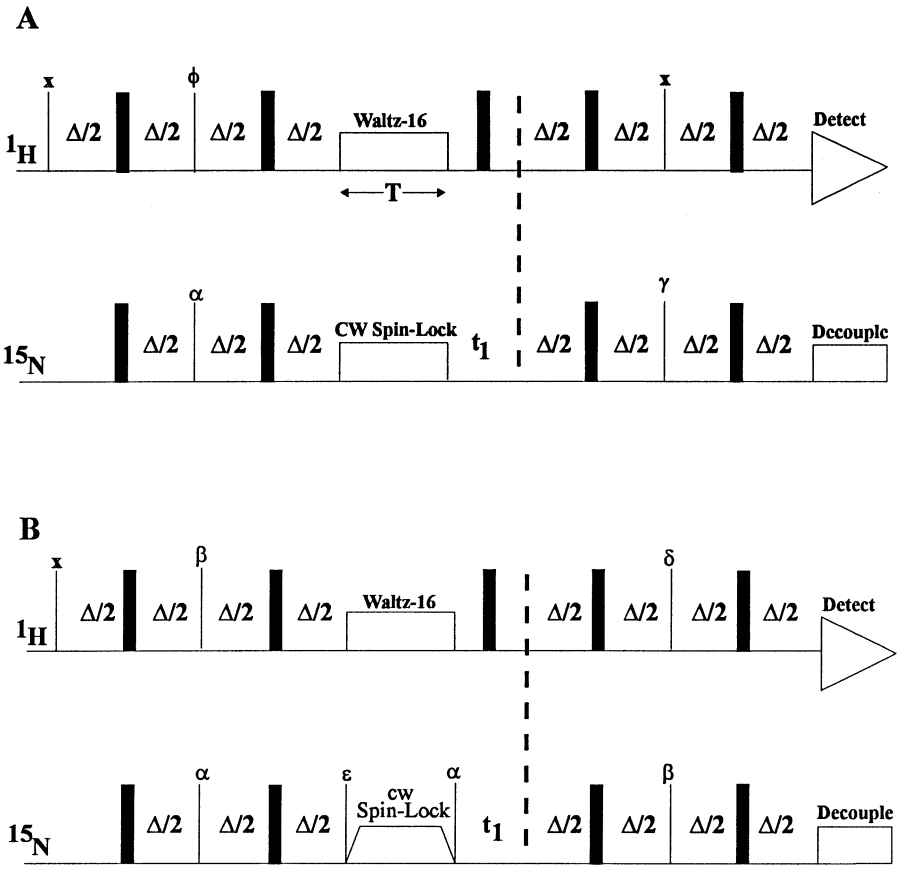

Figure 1. Two-dimensional heteronuclear pulse sequences for measuring the rotating-frame ^{15}N relaxation rate on- ($R_{1\rho}^{\mathrm{ON}}$, Fig. 1A) (Habazettl et al., 1996) and off-resonance ($R_{1\rho}^{\mathrm{OFF,cor}}$, Fig 1B) (Zinn-Justin et al., 1997). The upper trace indicates proton pulses while the lower trace indicates the ^{15}N spin pulses. Pulses of 90° and 180° are shown as thin and thick vertical bars, respectively. In the pulse sequence of Figure 1A, the TPPI phase modulation is done on the first 90° ^{15}N pulse following the t_1 period. In the pulse sequence of Figure 1B, the TPPI phase modulation is done on the 90° ^{15}N pulse immediately after the shaped cw spin-lock period. Pulse phases are shown above the pulses themselves with $\alpha = +x, -x$; $\phi = 4(+y), 4(-y)$; $\beta = +y, +y, -y, -y$, $\gamma = +x, +x, -x, -x$, $\delta = 4(+x), 4(-x)$, $\epsilon = +y, -y, -y, +y, +y, -y, -y, +y, -y, +y, +y, -y, -y, +y, +y, -y$. In both sequences, Waltz-16 composite pulse decoupling was applied on the protons during the continuous wave spin lock of the ^{15}N magnetization. The continuous wave spin-lock strength was varied. In the pulse sequence shown in Figure 1B, the field was increased and decreased gradually (in 2.5 ms) so that the magnetization components are rotated adiabatically.

NMR experiments

All NMR experiments were carried out at 15 °C, on a Bruker DRX 500 NMR spectrometer operating at a proton Larmor frequency of 500.13 MHz.

The on-resonance rotating-frame relaxation rate ($R_{1\rho}^{\mathrm{ON}}$) is measured as a function of the spin-lock field strength (ω_1) by using a recently published pulse sequence (Habazettl et al., 1996) which is also shown in Figure 1A. In this experiment, the carrier of the spin-lock field is set on resonance with the nitrogen resonance frequency of the residue of interest. During the application of the continuous wave spin-lock field at the ^{15}N channel, decoupling of the protons is achieved with Waltz-16 (Shaka et al., 1983) in order to avoid creation of antiphase ^{15}N magnetization (of the type $N_x I_z$, where N and I are the nuclear spin operators of the ^{15}N and the directly bound ^{1}H nucleus, respectively) via cross-correlation processes. The decoupling power was equal to 3390 Hz. The INEPT transfer delay was set to 2.5 ms. The effective spin-lock magnetic field amplitudes (effective field amplitude hereafter) used for the measurement of $R_{1\rho}^{\mathrm{ON}}$ were the following: 1170, 1280, 1570, 1920, 2110, and 2310 Hz. For each effective field amplitude, a series of 2D experiments were performed in which

the relaxation delay, T, corresponding to the duration of the application of the spin lock field was varied as follows: 10, 20, 36, 50, 60, 86, 100, 150, 200, 300, and 5 ms. All experiments were recorded with a spectral width of 7003 Hz in the F_2 dimension (^{1}H frequency) with the carrier placed on the water signal. In the F_1 dimension (^{15}N frequency) the spectral width was set equal to 2500 Hz. A total of 128 experiments in t_1, each of 2048 real data points, were recorded. Every free induction decay was comprised of 16 scans. The measuring time for every 2D spectrum was approximately 1 hour. Quadrature detection in F_1 was obtained by using the TPPI method of Marion and Wuthrich (1983).

The measurement of $R_{1\rho}$ was also done by using a non-zero offset value ($= \Delta\omega$) between the carrier and the resonance frequencies. The pulse sequence used was the one described in Zinn-Justin *et al.* (1997) and is shown in Figure 1B. As can be seen, a trapezoid-shaped spin-lock pulse is applied in order to achieve adiabatic rotation of the *z*-magnetization by an angle θ (chosen to be equal to 35° in our case). This relaxation rate is denoted $R_{1\rho}$ off resonance, $R_{1\rho}^{\mathrm{OFF}}$. The effective field amplitude values employed for the measurement of $R_{1\rho}^{\mathrm{OFF}}$ were the following: 2230, 2740, 3020, 3340, 3680, 4030, 4470 Hz. As also described in the preceding paragraph, a series of 2D spectra were acquired for each effective field amplitude value by varying the duration of the spin lock shaped pulse as follows: 10, 20, 36, 50, 60, 86, 100, 150, 200, 300 and again 10 ms. The acquisition parameters of this series of 2D data were identical to the ones used for the measurement of $R_{1\rho}^{\mathrm{ON}}$, with the difference that the carrier frequency in the F_1 dimension was set approximately in the center of the amide nitrogen region. In addition, when measuring both $R_{1\rho}^{\mathrm{ON}}$ and $R_{1\rho}^{\mathrm{OFF}}$, an extra 2D spectrum was obtained by setting $\mathrm{T} = 2\ \mu\mathrm{s}$. This was done in order to have a measure of the magnetization at the beginning of the time period.

The longitudinal relaxation rate, R_1, was measured as described in Peng and Wagner (1994) by using the following delays: 10, 20, 40, 80, 120, 240, 320, 500, 1000, and 1500 ms. The acquisition parameters were equivalent to the ones used for the measurement of $R_{1\rho}^{\mathrm{OFF}}$ except that a total of 192 experiments in t_1 were recorded, each being comprised of 8 scans.

For cross-peak assignment, we used the recently published sequence specific assignment of the ^{1}H and ^{15}N NMR spectra of reduced recombinant HiPIP I from *E. halophila* (Bertini et al., 1994).

Data Processing

All 2D NMR data were processed on an INDY SLC workstation using the Xwinnmr Bruker software. Only the downfield part of the spectra (in the ^{1}H dimension), containing the H_N–N connectivities (5–12 ppm), were kept for the data analysis. All spectra acquired with a common effective field amplitude value were processed by using the same processing parameters (2K × 512 points in the F_2 and F_1 dimensions respectively, phasing parameters, baseline correction, etc.). Subsequent integration of cross peaks for all spectra was performed by using the standard routine available from Bruker.

Determination of Relaxation Rates

For the determination of the relaxation rates R_1, $R_{1\rho}^{\mathrm{OFF}}$ and $R_{1\rho}^{\mathrm{ON}}$ the cross-peak intensities (I) measured as a function of the relaxation delay T, were fit to a single exponential decay by using the Levenberg-Marquardt algorithm (Marquardt, 1963; Press et al., 1988) according to the following equation:

$$\mathrm{I(T)} = A + B \cdot \exp[-R\mathrm{T}] \qquad (1)$$

A and B and R were used as adjustable fitting parameters. For $R_{1\rho}^{\mathrm{ON}}$, since the magnetization should relax to zero, A was set equal to zero in the fitting procedure. The same was done also for $R_{1\rho}^{\mathrm{OFF}}$ because the sequence phase cycle was chosen so that the magnetization relaxes to zero for long relaxation delays. The error bars correspond to the experimental error averaged over all effective field amplitudes. This error value includes the errors in the measurement of both $R_{1\rho}^{\mathrm{OFF}}$ and R_1. The fitting was done with a program kindly provided by Dr H. Desvaux. In order to estimate the uncertainty in the values extracted for R, the program uses a Monte Carlo approach similar to the one previously used by several researchers (Palmer, III et al., 1991; Peng and Wagner, 1992; Zinn-Justin et al., 1997).

Methodology

Rotating frame ^{15}N relaxation

The relaxation rate $R_{1\rho}^{\mathrm{ON}}$, provided the system is in the limit of fast (chemical and/or conformational) exchange between two conformations, i.e. $\delta\Omega \cdot \tau_{\mathrm{ex}} \ll 1$, where $\delta\Omega$ is the chemical shift difference between the two exchanging sites and τ_{ex} is the correlation time for

the exchange process, is described by the following equation (Deverell et al., 1970):

$$R_{1\rho}^{\mathrm{ON}} = R_{1\rho}^{\mathrm{ON},\infty} + K \cdot \frac{\tau_{\mathrm{ex}}}{1 + \tau_{\mathrm{ex}}^2 \cdot \omega_1^2} \qquad (2)$$

where ω_1 is the effective spin-lock magnetic field applied at the Larmor frequency ω_{i} of the spin i of interest, $R_{1\rho}^{\mathrm{ON},\infty}$ is the $R_{1\rho}^{\mathrm{ON}}$ relaxation rate for an infinitely large effective field amplitude ω_1 (where all the exchange contributions are dispersed to zero), τ_{ex} is the time constant for the exchange process observed for the i^{th} spin, K is a constant equal to $p_a \cdot p_b \cdot \delta\Omega^2$, where p_a and p_b are the relative populations of the two states a and b between which the exchange process occurs.

If the RF irradiation is applied off-resonance with an offset $\Delta\omega_i = \omega_{\mathrm{rf}} - \omega_i$, where ω_{rf} is the RF frequency, then $R_{1\rho}^{\mathrm{OFF}}$ of the i^{th} spin is given by the following expression (Davis et al., 1994; Desvaux et al., 1995; James et al., 1977; Akke and Palmer, III, 1996):

$$\begin{aligned} R_{1\rho}^{\mathrm{OFF}} &= R_1 \cdot \cos^2\theta_i + R_{1\rho}^{\mathrm{ON},\infty} \cdot \sin^2\theta_i \\ &\quad + K \cdot \sin^2\theta_i \cdot \frac{\tau_{\mathrm{ex}}}{1 + \tau_{\mathrm{ex}}^2 \cdot \omega_{\mathrm{eff},i}^2} \end{aligned} \qquad (3)$$

where R_1 is the longitudinal relaxation rate of the i^{th} spin, $\theta_i = \arctan(\omega_1/\Delta\omega_i)$ and $\omega_{\mathrm{eff},i} = (\Delta\omega_i^2 + \omega_1^2)^{1/2}$. The above equation can be rearranged as follows:

$$\begin{aligned} &\frac{R_{1\rho}^{\mathrm{OFF}} - R_1 \cdot \cos^2\theta_i}{\sin^2\theta_i} = \\ &\qquad R_{1\rho}^{\mathrm{ON},\infty} + K \cdot \frac{\tau_{\mathrm{ex}}}{1 + \tau_{\mathrm{ex}}^2 \cdot \omega_{\mathrm{eff},i}^2} \end{aligned} \qquad (4)$$

The first term of the above equation can be defined as the corrected off-resonance relaxation rate and will be referred to as $R_{1\rho}^{\mathrm{OFF,cor}}$ hereafter. Note that the latter quantity corresponds to $R_{1\rho}$ measured at $\omega_{\mathrm{eff},i}$ with $\vartheta_i = 90°$, i.e. $R_{1\rho}^{\mathrm{ON}}$. If $R_{1\rho}^{\mathrm{OFF}}$, R_1, θ_i are known, then $R_{1\rho}^{\mathrm{OFF,cor}}$ can be calculated.

By comparing Equations 2 and 4 and taking into account that in the on-resonance case, $\omega_{\mathrm{eff},i} = \omega_1$, it can be noted that the value of $R_{1\rho}^{\mathrm{OFF,cor}}$ at a given effective field amplitude $\omega_{\mathrm{eff},i}$ is equal to the value of $R_{1\rho}^{\mathrm{ON}}$ at the same effective field amplitude. Therefore the data of the two sets of experiments, i.e. $R_{1\rho}^{\mathrm{ON}}$ and $R_{1\rho}^{\mathrm{OFF,cor}}$, can be fitted simultaneously to a single equation. This allows us to expand the experimentally available range of effective spin-lock field strengths and consequently the time regime for the exchange processes observed. Equations 2 and 4 show that the dependence of $R_{1\rho}^{\mathrm{ON}}$ or $R_{1\rho}^{\mathrm{OFF,cor}}$ on ω_{eff}, is indicative of the presence of an exchange process involving the backbone nitrogen. By fitting the experimental points to a Lorenzian (Equation 2 or 4), the time constant τ_{ex} associated with the exchange process can be extracted. If on the other hand, no exchange process is present, $R_{1\rho}^{\mathrm{OFF,cor}}$ (and $R_{1\rho}^{\mathrm{ON}}$) are independent of ω_{eff}. It should be noted that the strict division between on- and off-resonance rotating frame relaxation is artificial, since the variation from on- to off-resonance occurs gradually as the offset differs from zero. One of the aims of this study is to show that the combination of on- and off-resonance RF irradiation can be very useful to identify 'slow motions' in proteins. Despite it being artificial, we will maintain the above classification in the $R_{1\rho}$ data ($R_{1\rho}^{\mathrm{ON}}$, $R_{1\rho}^{\mathrm{OFF}}$) to refer to the two different experimental pulse sequences.

The experimentally accessible time regime is directly dependent on the effective field amplitude range available by the NMR probe (Desvaux et al., 1995). In the presence of a 'fast' process ($\tau_{\mathrm{ex}} < 1/\omega_{\mathrm{eff}}$), the third term of Equation 2 equals $K \cdot \tau_{\mathrm{ex}}$. Thus $R_{1\rho}^{\mathrm{OFF}}$ appears to be constant as a function of ω_{eff} but larger than in the absence of an exchange process and equal to $R_{1\rho}^{\mathrm{ON},\infty} + K \cdot \tau_{\mathrm{ex}}$. In this limit, however, the exact value of τ_{ex} cannot be accurately estimated because K is not known. The term $K \cdot \tau_{\mathrm{ex}}$ depends on the square of the chemical shift difference ($\delta\Omega^2$) between the two conformations. However, the chemical shift is known to be very sensitive to conformational changes and thus a motion with a significant amplitude is expected to have a non-negligible value of $\delta\Omega$. In the case of a motion associated with a small $\delta\Omega$, the contribution of exchange to $R_{1\rho}$ is too small to be detected irrespective of the timescale of the motion.

Effect of the paramagnetic center

The presence of a paramagnetic center provides additional contributions to nuclear relaxation via the dipolar and contact interactions as well as the interaction with the Curie spin. In the present system, only the dipolar contribution is operative, since no ^{15}N nuclei experience contact interaction, all being separated from the paramagnetic center by more than four bonds. The Curie contribution is also small in

this case (Bertini et al., 1996a). In previous works (Bertini et al., 1996b; Bertini et al., 1996a) the effect of the paramagnetic center (ρ_i^{para}) on longitudinal proton relaxation, due to dipolar coupling with the metal cluster, has been accounted for by the Solomon equation (Solomon, 1955), which can be expressed by the following relation:

$$\rho_i^{para} = \sum_{f=1}^{4} \frac{K_H}{r_{if}^6} \tag{5}$$

where the sum extends over the four iron atoms (f) constituting the cluster, r_{if} is the distance of the i proton from the iron f and K_H is a constant that has been experimentally determined (Bertini et al., 1996b; Bertini et al., 1996a) and includes all the other relevant electronic parameters (multiplicity of the electron spin states, the electron relaxation times) and physical constants (including γ_H). Due to the size of the molecule, the correlation time for the interaction with the paramagnetic center is determined by the relaxation time of the electron spin. Since the situation in a coupled system is largely complicated at room temperature due to the population of several electronic levels, a unique value for the effective electronic correlation time (τ_s) cannot be evaluated. The K_H constant, however, can be scaled by a factor of $(\gamma_N/\gamma_H)^2$ and used to estimate the paramagnetic contribution to the longitudinal relaxation of the nitrogen spins. On the contrary, we do not have any experimental information on the paramagnetic contribution to transverse relaxation and, by not knowing τ_s, it cannot be calculated. Therefore we can only estimate a lower limit for the paramagnetic contribution to transverse relaxation, equal to the longitudinal one.

Like all other terms contributing to nuclear relaxation except chemical exchange, the paramagnetic term is independent of the effective field amplitude. Thus, exchange processes can be also probed in the presence of a paramagnetic center.

Results

Relaxation Rates $R_{1\rho}^{OFF,cor}$ and $R_{1\rho}^{ON}$.

An example of a representative ^{1}H–^{15}N 2D spectrum obtained for the measurement of $R_{1\rho}^{OFF}$ is shown in Figure 2. In this spectrum, an effective spin-lock field of 2230 Hz was employed for a period of 10 ms. The off-resonance rotating frame relaxation rate, $R_{1\rho}^{OFF}$, was determined for each amide backbone ^{15}N resonance at seven different amplitudes of the effective RF field, ω_{eff}. Subsequently, the experimental values of $R_{1\rho}^{OFF}$ were corrected for the angle θ_i.

In our case, off-resonance experiments were performed by simultaneously changing the values of ω_1 and $\Delta\omega_j$ (for the resonance j located in the center of ^{15}N resonances) so that the ratio of $\omega_1/\Delta\omega_j$ (and therefore θ_j) is kept constant in order to have $\theta_j = 35°$. For all other ^{15}N resonances (i), the angle θ_i will undergo a small but systematic variation with the corresponding increase of ω_1 and $\Delta\omega_j$. However, this is accounted for by using Equation 4. In the specific case of the protein HiPIP I examined in this work, the largest increase in θ_i between the lowest and highest values of ω_1 used was 3.3° (for the NH resonance of residue 46). The corresponding largest decrease was 4.7° (for the NH resonance of residue 18). It should be noted, however, that the angular dispersion in the tilted rotating frame (off-resonance) is always smaller than the corresponding dispersion when on-resonance RF irradiation is applied.

The dependence of $R_{1\rho}^{OFF,cor}$ on ω_{eff} was carefully examined for each amide backbone resonance separately. It was concluded that for all amide resonances with the exception of one (NH of Gln 44), the values of $R_{1\rho}^{OFF,cor}$ were independent of the effective field amplitude used. The average values of $R_{1\rho}^{OFF,cor}$ (estimated using all the values obtained at the seven effective field amplitudes employed in the experiments) of each NH backbone resonance along the protein sequence are shown in Figure 3. The rates of 51 residues in total are displayed. These correspond to resonances that are well resolved in the 2D NMR spectra so that they can be precisely integrated.

The paramagnetic relaxation rate enhancement on the R_1 of the protons has been experimentally determined by Bertini et al. (1996a). It was shown that the effect of the metal cluster on R_1 is negligible for metal to proton distances longer than 7 Å. This effect is scaled down by a factor of about 100 for the nitrogen relaxation rates due to the lower magnetogyric ratio of the ^{15}N nucleus. Therefore, all residues at distances greater than 7 Å from the metal center can be considered diamagnetic and analyzed as such. Of the detected residues, 12 are located at distances less than 7 Å from the polymetallic center. These are 14, 33–37, 40, 50, 60–61, 64, 67. We will present here all the results, but the corrections necessary for these 12 residues will be discussed in detail later. The

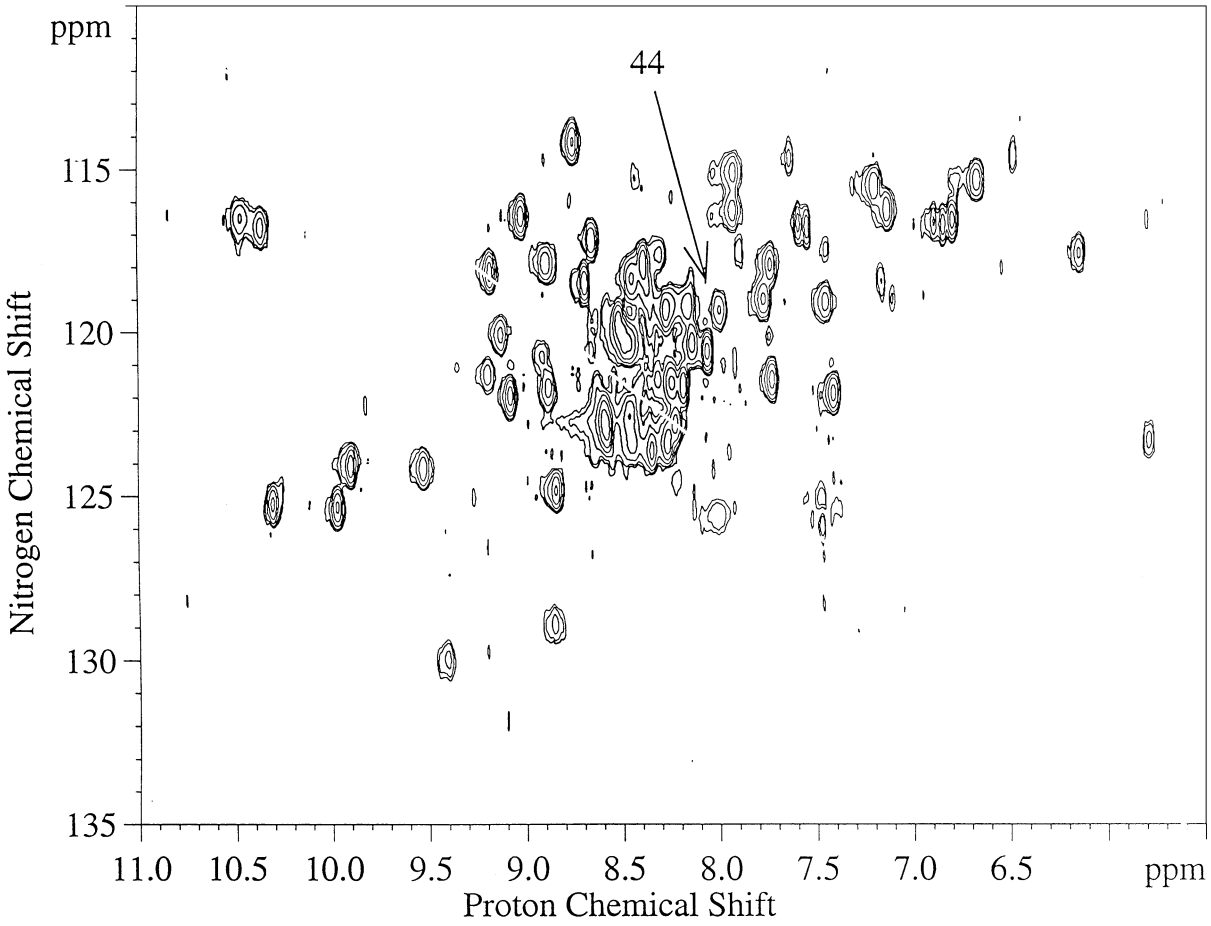

Figure 2. Representative ^{15}N–^{1}H 2D spectrum of the reduced form of HiPIP I from *E. halophila* obtained by using the pulse sequence of Figure 1B. An effective spin-lock field of 2230 Hz was employed for a period of 10 ms. The cross-peak indicated by an arrow is due to the backbone amide nitrogen ^{15}N of Gln 44. The full assignment of the cross-peaks has been published elsewhere (Bertini et al., 1994).

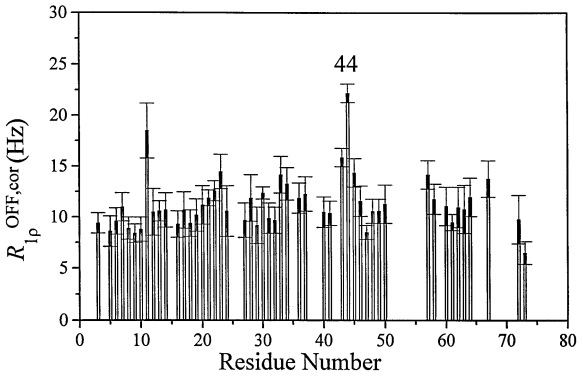

Figure 3. Bar graph of the experimental ^{15}N $R_{1\rho}^{OFF,cor}$ values versus the amino acid sequence for the reduced form of HiPIP I from *E. halophila* recorded at 500 MHz and 15 °C. The values displayed are the averages over the seven effective field amplitudes used, with the exception of Gln 44 whose value obtained at the lowest effective field amplitude is displayed (see Text for explanation).

rate reported in Figure 3 for the residue Gln 44 is not the average, but the value obtained at the lowest effective field amplitude (see below). The relaxation rates $R_{1\rho}^{OFF,cor}$ show a distinctly different behavior at residues 11, 22–23, 30, 43–45, 57 and 73 with respect to the other residues. Neglecting these residues as well as the 'paramagnetic' ones, the rates of the remaining 30 residues are quite uniform with an average value of $R_{1\rho}^{OFF,cor} = (10.1 \pm 1.5)$ Hz, which in this case equals $R_{1\rho}^{ON,\infty}$. According to the analysis presented in the Methodology section this could be interpreted in one of the following ways: (i) absence of an exchange process ($\tau_{ex} = 0$), (ii) presence of exchange processes with τ_{ex} larger than the reciprocal of the smallest ω_{eff} used, i.e. $\tau_{ex} > 150$ μs, (iii) $\delta\Omega$ is not large enough to contribute sizeably to $R_{1\rho}$.

Table 1. Average values of the rotating-frame ^{15}N relaxations rates $R_{1\rho}^{\mathrm{OFF,cor}}$ and $R_{1\rho}^{\mathrm{ON}}$ measured in the reduced HiPIP I from *E. halophila*

Residue	$R_{1\rho}^{\mathrm{OFF,cor}}$ (Hz)	$R_{1\rho}^{\mathrm{ON}}$ (Hz)
11	18 ± 3	16 ± 2
13	11 ± 1	12 ± 2
14	11 ± 2	10 ± 1
16	9 ± 1	9 ± 1
17	11 ± 2	10 ± 1
19	10 ± 2	10 ± 2
60	11 ± 2	10 ± 2
64	12 ± 2	13 ± 2

According to the presentation under Methodology, these $R_{1\rho}^{\mathrm{OFF,cor}}$ rates are equal to the corresponding rates on resonance when measured at the same effective field amplitude. By measuring the $R_{1\rho}^{\mathrm{ON}}$ for each resonance, direct experimental proof can be provided of this fact. We thus measured $R_{1\rho}^{\mathrm{ON}}$ as a function of effective field amplitude for residues 11, 13, 14, 16, 17, 19, 60 and 64. These specific residues were selected because they give rise to three groups of resonances with very similar ^{15}N chemical shift values: 14–19–60, 16–17, 11–13–64. Thus, it is possible to measure their $R_{1\rho}^{\mathrm{ON}}$ simultaneously for each group. The $R_{1\rho}^{\mathrm{ON}}$ rates for the above eight residues showed no dependence on the effective field amplitude employed and their average values are reported in Table 1, together with those of $R_{1\rho}^{\mathrm{OFF,cor}}$. As evidenced in Table 1, the two sets of rates are very similar, within experimental error, thus confirming the reliability of the treatment summarized in the 'Methodology' section.

Residues 11, 43, 45 and 57 have $R_{1\rho}^{\mathrm{OFF,cor}}$ rates (Figure 3) which are 40–80 % larger than those of the rest of the protein. By taking into account Equations (2) and (4), this behaviour is an indication of the presence of a conformational exchange process. However, its time scale is faster than the one accessible with the available amplitudes of the effective magnetic field (ω_{eff}) and thus, as discussed in the 'Methodology' section, $R_{1\rho}^{\mathrm{OFF,cor}}$ appears to be constant as a function of ω_{eff} but with a higher value than in the absence of an exchange process. Since the highest ω_{eff} available equals 4470 Hz, the exchange process operative for residues 11, 43, 45 and 57 should have a correlation time $\tau_{\mathrm{ex}} < 35$ μs and a value of $\delta\Omega$ that is large enough so that $K \cdot \tau_{\mathrm{ex}}$ is not negligible with respect to $R_{1\rho}^{\mathrm{ON},\infty}$ (10.1 ± 1.5 Hz). The use of higher ω_{eff} values would allow precise quantitation of such rapid exchange processes. This could be achieved by using larger resonance offsets, as previously reported (Akke et al., 1998). Among these four residues, the backbone nitrogen of Ala 11 displays the largest $R_{1\rho}^{\mathrm{OFF,cor}}$. The NH of Ala 11 is located 9.4 Å away from the closest iron atom and in an external loop, which excludes the possibility that the increased rotating-frame relaxation rates are due to paramagnetic effects. Its increased $R_{1\rho}^{\mathrm{OFF,cor}}$ value is therefore due to increased mobility, which is consistent with its structural features.

By knowing the average value of R_1 and the average value of $R_{1\rho}^{\mathrm{OFF,corr}}$ for the backbone nitrogens of all residues that are not involved in exchange processes, if we approximate $R_{1\rho}^{\mathrm{OFF,corr}} = R_2$, the overall rotational correlation time, τ_c, of the protein can be determined from the ratio R_2/R_1 (Kay et al., 1989). As described in the literature (Kay et al., 1989; Habazettl et al., 1996) the ratio R_2/R_1 is related with the ratio of the spectral densities $J(0)$ and $J(\omega_{\mathrm{N}})$ via the relation:

$$\frac{R_2}{R_1} \approx \frac{2}{3} \cdot \frac{J(0)}{J(\omega_N)} + \frac{1}{2}, \tag{6}$$

where $\omega_{\mathrm{N}} \approx 50.7$ MHz and it holds that

$$\frac{J(0)}{J(\omega_N)} = 1 + \omega_N^2 \tau_c^2. \tag{7}$$

By taking into account that the average values of $R_{1\rho}^{\mathrm{OFF,cor}}$ ($= R_2$) and R_1 for all ^{15}N resonances that display uniform relaxation rates in the rotating frame are 10.1 ± 1.5 Hz and 2.3 ± 0.2 Hz respectively, we can determine a value for $\tau_{\mathrm{c}} = 6.8 \pm 1.0$ ns.

Conformational Exchange Rate of Gln-44

The off-resonance rotating frame relaxation rate, $R_{1\rho}^{\mathrm{OFF,cor}}$, for the backbone nitrogen resonance of Gln 44 was the only one that displayed a dependence on ω_{eff}. The rates are shown in Figure 4 with solid symbols.

In order to obtain data points on a wider range of ω_{eff}, also measurements of $R_{1\rho}^{\mathrm{ON}}$ for the backbone nitrogen resonance of Gln 44 were performed as a function of ω_{eff}. The data points obtained are shown in Figure 4 with open symbols. It can be seen that, in the overlapping range of the values of ω_{eff} employed in the off- and on-resonance measurements, the

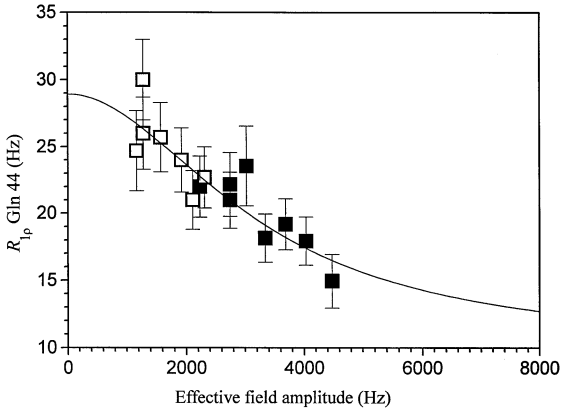

Figure 4. Plot of the experimental rotating-frame ^{15}N relaxation rate ($R_{1\rho} = R_{1\rho}^{\mathrm{ON}}$ or $R_{1\rho}^{\mathrm{OFF,cor}}$) of Gln-44 measured on- ($R_{1\rho}^{\mathrm{ON}}$) and off-($R_{1\rho}^{\mathrm{OFF,cor}}$) resonance as a function of the effective field amplitude (ω_{eff}). The open symbols correspond to $R_{1\rho}^{\mathrm{ON}}$ (measured with the pulse sequence 1A) and the solid symbols represent $R_{1\rho}^{\mathrm{OFF,cor}}$ (measured with the pulse sequence 1B). The solid curve represents the fit with the function of Equation 4 done by using the Levenberg–Marquardt algorithm. All experimental data points displayed were used for the fit.

rates of $R_{1\rho}^{\mathrm{OFF,cor}}$ are reproducible. In addition, the on-resonance data show a dependence on ω_{eff}, already evident from the off-resonance measurements.

The fit, performed on all the experimental values by using Equation 4, is superimposed on the experimental data in Figure 4 with a solid line. It was done by using the Levenberg-Marquardt algorithm (Marquardt, 1963; Press et al., 1988) and the errors calculated correspond to a confidence band of 95.6 %. In this fit, a fixed value of $R_{1rho}^{\mathrm{ON},\infty}$ was used ($R_{1\rho}^{\mathrm{ON},\infty} = 10.1$ Hz as estimated above), while K and τ_{ex} were adjustable parameters. This nonlinear fitting procedure provided a value of τ_{ex} for the backbone nitrogen of Gln-44 of 50 ± 6 μs and for the parameter K a value of $(3.8 \pm 0.2) \times 10^6$ s^{-2}. The fits were repeated by fixing the parameter $R_{1\rho}^{\mathrm{ON},\infty}$ to its upper and lower limits (11.6 and 8.6 Hz respectively) and they gave values for τ_{ex} and K within a 10–15% range from those obtained by using $R_{1\rho}^{\mathrm{ON},\infty} = 10.1$ Hz. By taking into account the results of all these three independent fits the final values for the parameters K and τ_{ex} are $(3.8 \pm 0.3) \times 10^6$ s^{-2} and 50 ± 8 μs, respectively. By assuming two equally populated states a and b between which the exchange process occurs ($p_a = p_b = 0.5$), this value of K corresponds to a chemical shift difference of 3.9 ± 0.3 ppm between the two exchanging conformations. When the fits are done independently on the two different data sets we obtain values of 50 ± 15 μs and 53 ± 17 μs for τ_{ex}, by using the $R_{1\rho}^{\mathrm{OFF,cor}}$ and $R_{1\rho}^{\mathrm{ON}}$ data, respectively. These values are identical, within experimental error, with the one determined by the simultaneous fit in both data sets, thus reconfirming the validity of the approach used. It is worth recalling that residues 43 and 45, adjacent to Gln-44, also experience conformational exchange, as discussed in the previous section. Even though we are not in a position to define the τ_{ex} parameter for these two residues, their time constant for the exchange process in which they participate has an upper limit of about 35 μs. This value is of the same order of magnitude of that estimated for Gln-44.

Discussion

In the present study, measurements of rotating frame ^{15}N backbone relaxation rates of the reduced recombinant HiPIP I from *E. halophila* were performed in order to probe molecular motions in the μs to ms time range. Such a 'slow' dynamic mode was identified in the external loop made up by residues 43–45.

The X-ray crystal structure of this protein has been solved at 2.5 Å resolution (Breiter et al., 1991). In that study it was seen that, although most of the electron density was well-ordered, the region around amino acids 40–46 presented difficulties in the fitting process because these residues adopted different conformations due to crystal packing. Indeed the two different molecules present in the crystal cell show different conformations in this region (Breiter et al., 1991). In the solution structure of the protein (Banci et al., 1994; Bertini et al., 1996a) residues 44–46 have average backbone RMSD values 60–70 % higher than the global average RMSD. The lower definition of this region could then be an indication of increased local mobility. Recently, Bertini et al. (1996b) used complete relaxation matrix analysis for further refinement of the solution structure of this protein. During these calculations it was observed that some consistent violations arose from residue 44 and it was thus speculated that 'this may be due to local mobility', for which the static model used in that study could not account for. Our results are in agreement with these NOE observations. Indeed, the observed reduced NOE intensities could be the result of exchange between two conformations. In general, the results presented in this work are consistent with all the above described, previously observed, experimental facts and provide

the first solid experimental evidence for the existence of conformational flexibility for the residues 43–45.

For all characterized HiPIPs it was noted that they have a fairly conserved tertiary structure, despite their quite different primary sequences. This holds especially for the cluster and its surroundings. However, their redox potentials display a large variation in the range of 50 to 450 mV (Przysiecki et al., 1985). Thus, in our effort to understand the factors controlling the redox potential in HiPIPs we should focus our attention on the protein regions that are different in the various isoenzymes. The loop that mostly varies among the different HiPIP structures is that connecting the second cysteine to the third, which in the present protein are Cys 36 and Cys 50. The finding of an exchange process in this loop indicates that there are two conformations accessible at room temperature. This could be important for electron transfer and for protein stability.

As already mentioned in the 'Introduction' the effect of the paramagnetic center on proton relaxation is not negligible and it has been used to achieve additional proton-metal distance constraints and to refine the solution structure. The effect on nitrogen relaxation is dramatically reduced due to the lower magnetogyric ratio of the ^{15}N with respect to the ^{1}H nucleus. However, in the previous studies, the electron contribution to relaxation was used to estimate a metal nucleus distance, where the relationship between the rate and the distance is $1/r^6$, reducing the impact of experimental error on the derived distances which were used in the structure calculations only as upper distance limits. When, on the other hand, mobility is analyzed the relationship between the observed parameter (a rate) and the unknown one (the spectral density function at different frequencies) is linear and thus the need for accuracy of the correction for paramagnetic effects is more stringent. For example, the contribution on longitudinal nitrogen relaxation will be more than 1 Hz for nuclei at a distance less than 4 Å from at least one iron atom. This is much smaller than the contribution on protons (100 Hz in the same conditions), but it has to be compared with the 'diamagnetic' nitrogen relaxation rate which is 2.3 $\pm$ 0.2 Hz on average. More specifically, for nine out of the 12 ^{15}N nuclei which are at a distance less than 7 Å from at least one iron atom, the polymetallic center provides 3–8% paramagnetic relaxation enhancement with respect to an average diamagnetic R_1 value of 2.3 Hz. For residues 36 and 37 the enhancement is of the order of about 10%, while for residue 33 it is of the order of 30%. After subtraction of the estimated ρ^{para}, the values of R_1 for residues 33, 36 and 37 (3.9, 2.9 and 2.8 Hz respectively) become 3.2 $\pm$ 0.3, 2.7 $\pm$ 0.2 and 2.5 $\pm$ 0.2 Hz respectively. For the remaining nine residues the paramagnetic enhancement is much smaller and the R_1 rates measured were between 2.4 and 2.7 Hz. The paramagnetic relaxation rate enhancement on rotating frame relaxation rates cannot be evaluated as we do not have an estimate of the paramagnetic contribution to transverse relaxation provided by the metal center. However, we can provide a lower limit to this contribution, given by the ρ^{para}. Table 2 shows the $R_{1\rho}^{OFF,cor}$ values for the 12 residues at a distance less than 7 Å from at least one iron atom before and after subtracting the paramagnetic contribution.

Table 2. Average values of $R_{1\rho}^{OFF,cor}$ and the corresponding values after correction for the paramagnetic effect in the reduced HiPIP I from *E. halophila*

Residue	$R_{1\rho}^{OFF,cor}$ (Hz)	$R_{1\rho}^{OFF,cor} - \rho^{para}$ (Hz)
14	10.7 $\pm$ 1.7	10.6 $\pm$ 1.7
33	14.2 $\pm$ 1.8	13.5 $\pm$ 2.0
34	13.3 $\pm$ 1.6	13.1 $\pm$ 1.6
35	10.0 $\pm$ 1.5	9.9 $\pm$ 1.5
36	11.9 $\pm$ 1.5	11.7 $\pm$ 1.6
37	12.3 $\pm$ 1.7	12.0 $\pm$ 1.8
40	11.9 $\pm$ 2.2	11.8 $\pm$ 2.2
50	11.3 $\pm$ 1.9	11.1 $\pm$ 1.9
60	11.1 $\pm$ 1.9	11.0 $\pm$ 1.9
61	9.5 $\pm$ 0.8	9.4 $\pm$ 0.8
64	12.0 $\pm$ 1.9	11.8 $\pm$ 1.9
67	13.8 $\pm$ 2.0	13.6 $\pm$ 2.0

In conclusion, the effect of the paramagnetic, center on nitrogen relaxation can be partially accounted for by exploiting the available knowledge from longitudinal proton relaxation studies. The fact that a correction cannot be given for transverse relaxation with the present data, prevents the interpretation of self-relaxation rates in terms of local dynamics in the ps-ns time range. However, this does not prevent the observation of exchange phenomena in the µs-ms time range through the exploitation of rotating frame relaxation rates versus the effective field amplitude.

Another point that should be discussed concerns the determination of the overall rotational correlation time, τ_c, of the protein. By using the experimental data of this work τ_c is estimated to be 6.8 $\pm$

1.0 ns. However, in a recent study on the same protein where calculated and experimental NOE intensities were compared in order to account for the paramagnetic effect on their intensities (Bertini et al., 1996b), this correlation time was estimated to be 4 ± 1 ns. The upper limit of 5 ns is relatively close to the lower limit of 5.8 ns resulting from our work. An alternative approach to study the dynamics in the ps-ns timescale has been recently proposed (Felli et al., 1998). This approach is based on the measurement of cross correlation rates and yields the $J(W_N)/J(0)$ ratio. For the residues that did not show any modes faster than τ_c, the ratio was 7.55 ± 1.60 which provides a value for τ_c 5.6 ± 0.7 ns. This value is very similar, within experimental error, to the one estimated in this work.

It is important to mention that the experimental methods of Felli et al. (1998) are not affected by exchange contributions and are 'silent' in the ms–μs time regime, while the opposite is true for the techniques used by us, which are tailored only to detect motions in this time range. Consequently, it is interesting to note that Felli et al. (1998) did not detect any 'fast' motional modes for residues 41–46 which is consistent with our results. We can thus conclude that the present study, together with that of Felli et al. (1998) provide valuable complementary information on the dynamic properties of the reduced recombinant high-potential iron sulfur protein I (HiPIP I) from *E. halophila* in two different time domains.

Acknowledgements

We wish to thank Dr H. Desvaux for providing us with a copy of the manuscript describing the pulse sequence shown in Figure 1B prior to publication, and also for providing the program to fit the experimental intensities. Prof. I. Bertini encouraged and stimulated us with helpful discussions. D. K. wishes to thank the TMR Programme of the European Union for a postdoctoral fellowship (Contr. No ERBFMBICT960994)

References

Abragam, A. (1961) in *The Principles of Nuclear Magnetism*, Oxford University Press, Oxford.

Akke, M., Liu, J., Cavanagh, J., Erickson, H.P., and Palmer, A.G., III (1998) *Nature Struct. Biol.* **5**, 55–59.

Akke, M. and Palmer, A.G., III (1996) *J. Am. Chem. Soc.* **118**, 911–912.

Banci, L., Bertini, I., Briganti, F., Luchinat, C., Scozzafava, A., and Vicens Oliver, M. (1991) *Inorg. Chem.* **30**, 4517–4524.

Banci, L., Bertini, I., Capozzi, F., Carloni, P., Ciurli, S., Luchinat, C., and Piccioli, M. (1993a) *J. Am. Chem. Soc.* **115**, 3431–3440.

Banci, L., Bertini, I., Ciurli, S., Ferretti, S., Luchinat, C., and Piccioli, M. (1993b) *Biochemistry* **32**, 9387–9397.

Banci, L., Bertini, I., Eltis, L.D., Felli, I.C., Kastrau, D.H.W., Luchinat, C., Piccioli, M., Pierattelli, R., and Smith, M. (1994) *Eur. J. Biochem.* **225**, 715–725.

Banci, L. and Pierattelli, R. (1995) in *Nuclear Magnetic Resonance of Paramagnetic Macromolecules. NATO ASI Series* (La Mar, G.N. Ed.) Kluwer Academic, Dordrecht, pp. 281–296.

Bartsch, R.G. (1978) *Methods Enzymol.* **53**, 329.

Bertini, I., Briganti, F., Luchinat, C., Scozzafava, A., and Sola, M. (1991) *J. Am. Chem. Soc.* **113**, 1237–1245.

Bertini, I., Capozzi, F., Ciurli, S., Luchinat, C., Messori, L., and Piccioli, M. (1992a) *J. Am. Chem. Soc.* **114**, 3332–3340.

Bertini, I., Capozzi, F., Luchinat, C., Piccioli, M., and Vicens Oliver, M. (1992b) *Inorg. Chim. Acta* **198–200**, 483–491.

Bertini, I., Campos, A.P., Luchinat, C., and Teixeira, M. (1993a) *J. Inorg. Biochem.* **52**, 227–234.

Bertini, I., Capozzi, F., Luchinat, C., and Piccioli, M. (1993b) *Eur. J. Biochem.* **212**, 69–78.

Bertini, I., Felli, I.C., Kastrau, D.H.W., Luchinat, C., Piccioli, M., and Viezzoli, M.S. (1994) *Eur. J. Biochem.* **225**, 703–714.

Bertini, I., Eltis, L.D., Felli, I.C., Kastrau, D.H.W., Luchinat, C., and Piccioli, M. (1995) *Chemistry - A European Journal* **1**, 598–607.

Bertini, I. and Felli I.C. (1995) La Chimica e l'Industria 9, 639–648.

Bertini, I., Couture, M.M.J., Donaire, A., Eltis, L.D., Felli, I.C., Luchinat, C., Piccioli, M., and Rosato, A. (1996a) *Eur. J. Biochem.* **241**, 440–452.

Bertini, I., Felli, I.C., Luchinat, C., and Rosato, A. (1996b) *Proteins Struct. Funct. Genet.* **24**, 158–164.

Bertini, I., Luchinat, C., and Rosato, A. (1996c) *Prog. Biophys. Mol. Biol.* **66**, 43–80.

Bertini, I., Donaire, A., Felli, I.C., Luchinat, C., and Rosato, A. (1997) *Inorg. Chem.* **36**, 4798–4803.

Breiter, D.R., Meyer, T.E., Rayment, I., and Holden, H.M. (1991) *J. Biol. Chem.* **266**, 18660–18667.

Carter, C.W.J., Kraut, J., Freer, S.T., Alden, R.A., Sieker, L.C., Adman, E.T., and Jensen, L.H. (1972) *Proc. Natl. Acad. Sci. USA* **69**, 3526–3529.

Davis, D.G., Perlman, M.E., and London, R.E. (1994) *J. Magn. Reson. Ser. B* **104**, 266–275.

Desvaux, H., Birlirakis, N., Wary, C., and Berthault, P. (1995) *Mol. Phys.* **86**, 1059–1073.

Deverell, C., Morgan, R.E., and Strange, J.H. (1970) *Mol. Phys.* **18**, 553–559.

Dickson, D.P.E., Johnson, C.E., Cammack, R., Evans, M.C.W., Hall, D.O., and Rao, K.K. (1974) *Biochem. J.* **139**, 105

Dickson, D.P.E., Johnson, C.E., Middleton, P., Rush, J.D., Cammack, R., Hall, D.O., Mullinger, R.N., and Rao, K.K. (1976) *J. Physique Colloq.* **37**, C6-171-C6-175.

Dunham, W.R., Hagen, W.R., Fee, J.A., Sands, R.H., Dunbar, J.B., and Humblet, C. (1991) *Biochim. Biophys. Acta* **1079**, 253–262.

Eltis, L.D., Iwagami, S.G., and Smith, M. (1994) *Protein Eng.* **7**, 1145–1150.

Felli, I.C., Desvaux, H., and Bodenhausen, G. (1998), *J. Biomol. NMR*, in press.

Habazettl, J., Myers, C., Yuan, F., Verdine, G., and Wagner, G. (1996) *Biochemistry* **35**, 9335–9348.

Hagen, W.R. (1992) *Adv. Inorg. Chem.* **38**, 165–222.

Hochkoeppler, A., Ciurli, S., Venturoli, G., and Zannoni, D. (1995) *FEBS Lett.* **357**, 70–74.
Jacquinot, J.F. and Goldman, M. (1973) *Physical Review B* **8**, 1944–1957.
James, T.L., Matson, G.B., Kuntz, I.D., and Fisher, R.W. (1977) *J. Magn. Reson.* **28**, 417–426.
James, T.L., Matson, G.B., and Kuntz, I.D. (1978) *J. Am. Chem. Soc.* **100**, 3590–3594.
James, T.L. and Sawan, S.P. (1979) *J. Am. Chem. Soc.* **101**, 7050–7055.
Jones, G.P. (1966) *Phys. Rev.* **148**, 332.
Kay, L.E., Torchia, D.A., and Bax, A. (1989) *Biochemistry* **28**, 8972–8979.
Led, J.J. and Nesgard, E. (1987) *Biochemistry* **26**, 183.
Marion, D. and Wüthrich, K. (1983) *Biochem. Biophys. Res. Commun.* **113**, 967–974.
Marquardt, D.W. (1963) *J. Soc. Ind. Appl. Math.* **11**, 431–441.
Middleton, P., Dickson, D.P.E., Johnson, C.E., and Rush, J.D. (1980) *Eur. J. Biochem.* **104**, 289–296.
Moss, T.H., Bearden, A.J., Bartsch, R.G., and Cusanovich, M.A. (1968) *Biochemistry* **7**, 1591–1596.
Mouesca, J.-M., Lamotte, B., and Rius, G.J. (1991) *Inorg. Biochem.* **43**, 251.
Mouesca, J.-M., Rius, G.J., and Lamotte, B. (1993) *J. Am. Chem. Soc.* **115**, 4714–4731.
Palmer, A.G., III, Rance, M., and Wright, P.E. (1991) *J. Am. Chem. Soc.* **113**, 4371–4380.
Peng, J.W., Thanabal, V., and Wagner, G. (1991) *J. Magn. Reson.* **82**, 82–100.
Peng, J.W. and Wagner, G. (1992) *Biochemistry* **31**, 8571–8586.
Peng, J.W. and Wagner, G. (1994) *Methods Enzymol.* **239**, 563–596.
Peng, J.W. and Wagner, G. (1995) *Biochemistry* **34**, 16733–16752.
Press, W.H., Flannery, B.P., Teukolsky, S.A., and Vetterling, W.T. (1988) in *Numerical Recipes in C – The Art of Scientific Computing*, Cambridge University Press, New York.
Przysiecki, C.T., Meyer, T.E., and Cusanovich, M.A. (1985) *Biochemistry* **24**, 2542–2549.
Rius, G.J. and Lamotte, B. (1989) *J. Am. Chem. Soc.* **111**, 2464–2469.
Shaka, A.J., Keeler, J., and Freeman, R. (1983) *J. Magn. Reson.* **53**, 313–340.
Solomon, I. (1955) *Phys. Rev.* **99**, 559–565.
Szyperski, T., Luginbuhl, P., Otting, G., Güntert, P., and Wüthrich, K. (1993) *J. Biomol. NMR* **3**, 151–164.
Tjandra, N., Kuboniwa, H., Ren, H., and Bax, A. (1995) *Eur. J. Biochem.* **230**, 1014–1024.
Wennerström, H. (1972) *Mol. Phys.* **1**, 69–80.
Zinn-Justin, S., Berthault, P., Guenneugues, M., and Desvaux, H. (1997) *J. Biomol. NMR* **10**, 363–372.